Astron. & Astrophys. 5, 355—371 (1970)

The Evolution of a Vibrationally Unstable Main-sequence Star of 130 $M_\odot$*

I. Appenzeller
Universitäts-Sternwarte Göttingen

Received December 19, 1969

Nonlinear pulsation calculations have been carried out for a 130 $M_\odot$ main-sequence star. For this purpose the dynamical equations of stellar structure were solved numerically using an implicit difference method. The main results are: during the first 20000 years (after the beginning of central hydrogen burning) the pulsation amplitude is too small to have any influence on the evolution of the star. After about 23000 years periodically recurring shock waves in the outer layers of the star result in the forming of an optically thick, continuously expanding shell around the star. Eventually the outermost layers of the shell reach the escape velocity and the star starts to loose mass at a maximum rate of about 4×10^{-5} $M_\odot$ per year. At this evolutionary stage the damping of the pulsations due to the loss of mechanical energy in the outer layers of the star becomes so large that the pulsation amplitude cannot increase any more. Thus, such a star is not destroyed rapidly by its vibrational instability (as suggested by earlier investigators), but a quasi-stationary state is reached, where the interior of the star is pulsating while the observable surface layers are expanding continuously. A comparison of the model calculations with the observed properties of the peculiar shell star P Cyg supports the hypothesis that P Cyg is a vibrationally unstable main-sequence star of $M > 100$ $M_\odot$.

Key words: stellar evolution — nonlinear pulsation — mass loss — P Cyg stars

I. Introduction

Because of the temperature dependence of the nuclear reaction rates mechanical energy is generated in the cores of pulsating main-sequence stars. In most main-sequence stars this gain of mechanical energy in the core is compensated by a much stronger loss of mechanical energy in the outer layers. Only in stars which are more massive than about 60 $M_\odot$ is more mechanical energy generated than is lost (Ledoux, 1941; Schwarzschild and Härm, 1959). Thus, these very massive main-sequence stars are vibrationally unstable. Since the instability increases strongly with increasing mass, Schwarzschild and Härm (1959) suggested that stars with $M > 100$ $M_\odot$ are destroyed by radial oscillations of rapidly increasing amplitude as soon as they reach the zero-age main-sequence phase of their evolution. However, this suggestion was based on the linear pulsation theory which is not valid for the large amplitude oscillations that are necessary to destroy such a star. Therefore, the fate of a very massive main-sequence star was reinvestigated using the exact nonlinear theory. As an example a 130 $M_\odot$ star was chosen. This mass is large enough to make the star strongly vibrationally unstable. On the other hand this seems still close enough to the largest stellar mass that has been determined directly so far (64 $M_\odot$ according to Sahade, 1962) to make it likely that stars of this mass do form occasionally. The scope of the new calculations was to find out if such a star will indeed be destroyed by rapid mass loss during its main-sequence evolution, or if the growth of the pulsation amplitude is halted by nonlinear effects before the star starts to eject large amounts of mass. In addition, it has been tried to determine how the observable properties of such a very massive main-sequence star are changed by the vibrational instability in order to make possible the identification of massive main-sequence stars from observations without determining directly their mass.

* Habilitationsschrift at the University of Göttingen

II. Basic Equations

The 130 $M_\odot$ star was assumed to be spherically symmetric and not rotating. Furthermore, since the pulsation amplitude is growing on a much shorter time scale than the nuclear time scale of the star, the chemical composition was assumed to be constant and equal to that of the zero-age main-sequence. For the relative mass fractions of hydrogen (X), helium (Y), and the heavier elements (Z) the values $X = 0.70$, $Y = 0.27$, and $Z = 0.03$ were chosen. Then, using the independent variables M_r (the mass contained within a sphere of radius r around the stellar center) and time t, and the dependent variables pressure $P(M_r, t)$, temperature $T(M_r, t)$, luminosity $L_r(M_r, t)$, radius $r(M_r, t)$ and the known functions internal energy per gram $U(P, T)$, specific volume $V(P, T)$, the nuclear energy generation per gram and second $\varepsilon_N(P, T)$, and the opacity $\varkappa$, a radially pulsating star can be described by the following four differential equations:

$$-4\pi r^2 \frac{\partial P}{\partial M_r} = \frac{\partial^2 r}{\partial t^2} + \frac{GM_r}{r^2} \tag{1}$$

(equation of motion, G is the gravitational constant),

$$\frac{\partial L_r}{\partial M_r} = \varepsilon_N - \frac{\partial U}{\partial t} - P\frac{\partial V}{\partial t} \tag{2}$$

(energy balance equation),

$$\frac{\partial r}{\partial M_r} = \frac{V}{4\pi r^2} \tag{3}$$

(equation of continuity),

$$L_r = -\frac{64\pi^2 ac\, r^4 T^3}{3\varkappa}\frac{\partial T}{\partial M_r} + L_{rc} \tag{4}$$

(energy transport equation; a is the radiation density constant, c the velocity of light).

The convective energy flux L_{rc} in Eq. (4) was assumed to be time independent and a function of M_r only. In a 130 $M_\odot$ star this is a good approximation, since the convective time scale is much larger than the pulsation period (Schwarzschild and Härm, 1959) and since in addition the periodic change of the acceleration of the convective elements due to the pulsation is small everywhere in the convective interior of the star, even when the velocity amplitude at the surface reaches the escape velocity. Thus, the absolute periodic variation of L_{rc} is always much smaller than the periodic variation of the radiative energy flux. Since in the convective core the mean values of P, T, L_r, and r averaged over one pulsation period depend only slightly on the pulsation amplitude and since the boundary of the central convective zone does not change, the numerical values of the function $L_{rc}(M_r)$ were taken from a hydrostatic 130 $M_\odot$ main-sequence stellar model. This model was derived using the standard stellar evolution computer program of Hofmeister, Kippenhahn and Weigert (1964). It was found to fit very well into the sequence of massive main-sequence stellar models of different mass computed by Stothers (1966). The basic properties of the hydrostatic 130 $M_\odot$ model are listed in the Table.

Table. *Basic properties of the hydrostatic 130 $M_\odot$ zero-age-main-sequence stellar model*

Radius R	1.033×10^7 km $\mathrel{\hat{=}}$ 14.9 $R_\odot$
Luminosity L	8.15×10^{39} erg s^{-1} $\mathrel{\hat{=}}$ $2.09 \times 10^6 L_\odot$
Effective temperature T_{eff}	57 100 °K
Central Pressure P_c	1.602×10^{16} dyn cm^{-2}
Central Temperature T_c	4.269×10^7 °K
Boundary of the convective core	$Mr/M = 0.878$

At large pulsation amplitudes thin convective zones develop at the boundaries of shock fronts. However, shock waves occur only in the outermost layers of the star where, because of the extremely low density, convective energy transport is very ineffective. Therefore the convective contribution to the energy transport in these zones was neglected.

In a 130 $M_\odot$ main-sequence star the gas pressure and the radiation pressure contribute about equal parts to the total pressure P. Thus the functions U and V become

$$U = \frac{2}{3}\frac{\mathcal{R}T}{\mu} + \frac{a}{\varrho}T^4 \tag{5}$$

and

$$V = \frac{\mathcal{R}T}{\mu}\left(P - \frac{a}{3}T^4\right)^{-1} \tag{6}$$

where $\mathcal{R}$ is the gas constant, μ is the mean molecular weight, and $\varrho = V^{-1}$ is the density.

The opacity was assumed to be due to electron scattering alone, or

$$\varkappa = 0.19\,(1 + X)\ \text{cm}^2\,\text{g}^{-1}\,. \tag{7}$$

In the core of a 130 $M_\odot$ main-sequence star all contributions to ε_N of nuclear reactions other than the CNO-cycle are negligible. Therefore for ε_N in Eq. (2) the expression for ε_{CNO} given by Hofmeister, Kippenhahn and Weigert [1964, Eq. (47)] was used.

III. Boundary Conditions

In the center of the star, at $M_r = 0$, the proper boundary conditions are obviously $L_r = 0$, $r = 0$, and $\partial r/\partial t = 0$. At the surface the correct boundary condition would be, to fit the values of P, T, and L_r at the bottom of a properly chosen stellar atmosphere to the solution of Eqs. (1) to (4). Since the atmosphere depends on the interior solution and vice versa the fitting usually requires an iterative procedure. In order to avoid time consuming iterative procedures and since the solutions do not depend critically on the outer boundary conditions rather approximate outer boundary conditions were used: at a value M_r

corresponding to the optical depth $\tau = 2/3$ the following two conditions were added to the basic differential equations:

$$L_r = 4\,\pi\, r^2\, \sigma\, T^4 \tag{8}$$

(where σ is the Stefan-Boltzmann constant) and

$$P = \frac{2}{3}\varkappa^{-1}\left(\frac{GM}{r^2} + \frac{\partial^2 r}{\partial t^2}\right) + \frac{a}{3}(0.812\; T)^4\,. \tag{9}$$

Equation (8) simply says that the temperature T at $\tau = 2/3$ is equal to the effective temperature. Equation (9) is derived by integrating analytically the equation of motion of the atmosphere

$$\frac{dP}{d\tau} = \varkappa^{-1}\left(\frac{GM}{r^2} + \frac{\partial^2 r}{\partial t^2}\right) \tag{10}$$

using the simplifying assumption that the right-hand side of Eq. (10) is independent of τ and that

$$P\,(\tau = 0) = \frac{a}{3}\, T^4\,(\tau = 0) = \frac{a}{3}\left(0.812\; T\left(\tau = \frac{2}{3}\right)\right)^4\,. \tag{11}$$

[The relation between $T\,(\tau = 0)$ and $T\,(\tau = 2/3)$ is taken from the theory of gray atmospheres.]

As a further simplification of the calculations it was assumed that the value M_r corresponding to $\tau = 2/3$ stays constant during the pulsations and equal to the value of the hydrostatic stellar model. For the quasi-periodic pulsations of the 130 $M_\odot$ star this is a sufficiently good approximation since according to Eq. (7) $\varkappa$ is a constant, since only about 10^{-10} of the stellar mass are outside $\tau = 2/3$, and since the relative radius variation $\delta R/R$ is always smaller than unity. When mass is ejected from the star, however, the simplified boundary conditions result in inaccurate or erroneous atmospheric properties. Even then, the dynamics of the star is, at first, influenced only very little. Only when the surface radius of the star grows to values much larger than the initial radius, does the error eventually become serious since then the approximate boundary conditions simulate a star with an atmosphere to which mass is added at a rapidly increasing rate. In this phase, however, other assumptions (like those made for $\varkappa$) become invalid too.

IV. The Numerical Integration Procedure

The nonlinear pulsation equations [Eqs. (1) to (4)] have been solved before for the outer layers of RR-Lyrae and δ-Cep stars using difference equations with explicit difference schemes (see e.g. Christy, 1964; Cox *et al.*, 1966). Since the relative pulsation amplitude in the deep interior of a 130 $M_\odot$ main-sequence star is not negligible as in an RR-Lyr star and since, furthermore, the energizing mechanism for the pulsations of very massive main-sequence stars is located in the hydrogen burning core, the pulsation equations in the present case have to be solved for the whole star. Thus, an explicit difference method is not suited for the present problem since the Courant-Friedrichs condition and the extremely high velocity of sound in the stellar core would require extremely short time steps. Therefore, an implicit difference method, the so called Henyey-method (Henyey *et al.*, 1958), was chosen for the numerical integration procedure. This method is used frequently for the numerical integration of the hydrostatic equations of stellar structure. Recently Bodenheimer (1968) has shown, that this method can also be applied to dynamical stellar collapse calculations. A main advantage of the Henyey method over other implicit methods is that a relatively small amount of computer storage space is needed. This was important for the present work since for most of the time only a medium size computer (IBM 7040) was available for the numerical calculations. An extensive description of the Henyey-method has been given by Kippenhahn, Weigert and Hofmeister (1967). This description was followed as closely as possible. Therefore, only those details of the calculations will be described here where the method had to be modified because of the different character of the basic equations.

Before the differential equations were replaced by finite difference equations two important modifications were made:

first, the second order time derivative in Eq. (1) was eliminated by adding a fifth differential equation

$$\frac{\partial r}{\partial t} = v \tag{12}$$

and a fifth dependent variable $v\,(M_r, t)$ as defined by Eq. (12). Furthermore, an artificial viscous pressure $Q\,(M_r, t)$ was added to the pressure in Eq. (1) in order to avoid the well known numerical difficulties which are encountered when finite difference equations are applied to hydrodynamic problems where shock waves occur (Richtmyer, 1957). With these two modifications, Eq. (1) takes the form:

$$-\,4\pi\, r^2\,\frac{\partial (P + Q)}{\partial M_r} = \frac{GM_r}{r^2} + \frac{\partial v}{\partial t}\,. \tag{13}$$

In order to avoid a spurious damping of the pulsations, Q was only used for the large amplitude pulsations and only in the outermost layers of the star (containing about 10^{-5} of the total stellar mass) where the shock waves occurred. In order to provide a smooth transition between the outer layers with $Q \neq 0$ and the interior with $Q = 0$, the artificial viscosity Q in the outer layers was defined in the following way:

$$Q = l^2 \varrho \left(3 \frac{v}{r} + \frac{1}{\varrho} \frac{\partial \varrho}{\partial t}\right)^2$$

$$\text{if} \quad v < 0 \quad \textit{and} \quad \left(3 \frac{v}{r} + \frac{1}{\varrho} \frac{\partial \varrho}{\partial t}\right) > 0\,, \tag{14a}$$

$$Q = l^2 \varrho^{-1} \left(\frac{\partial \varrho}{\partial t}\right)^2$$

$$\text{if} \quad v \geqq 0 \quad \textit{and} \quad \frac{\partial \varrho}{\partial t} > 0\,, \tag{14b}$$

$$Q = 0 \quad \text{in all other cases.} \tag{14c}$$

In (14a) and (14b) l is an arbitrary constant, having the dimension of a length and being of the same order of magnitude as the thickness of the mass shells near the shock fronts. In the computer program l was an input parameter which was adjusted so that the shock fronts were smoothed out to about to 2 to 4 mass steps.
(14a) is equivalent to

$$Q = l^2 \varrho\, r^2 \left(\frac{\partial\,(v/r)}{\partial r}\right)^2 . \tag{15}$$

The artificial viscosity as defined above is therefore a minor modification of the formulation suggested by von Neumann and Richtmyer (Richtmyer, 1957). For the present problem the formulation given by Eq. (14) has the advantage that towards the interior of the star Q becomes automatically very small or zero, since in the interior of a pulsating massive main-sequence star v/r depends very little on r (cf. eg. Fig. 1). This, however, obviously is necessary in order to obtain a smooth transition into the interior region of the star where we have $Q = 0$.

Because of numerical reasons which are described in the Appendix the artificial viscous pressure was not included in the mechanical work term (the third term on the right hand side) of Eq. (2). Neglecting the dissipation of mechanical energy by the artificial viscosity, on the other hand, would violate the law of energy conservation and result in wrong velocities of the shock fronts and thus in wrong results. Test calculations with Q included in Eq. (2) showed that during one time step almost all mechanical energy dissipated by the artificial viscosity is transformed into internal energy within the shock front (and not radiated away). Therefore the viscous energy dissipation was taken into account by the following method: for each time step Δt, first the five Eqs. (13), (2), (3), (4) and (12) were solved numerically. Then for each mass shell the viscous energy dissipation per gram stellar matter ΔE_Q was computed from

$$\Delta E_Q = -\,Q \frac{\partial V}{\partial t} \Delta t\,. \tag{16}$$

ΔE_Q was then added to the specific internal energy of the corresponding mass shells by properly increasing the values of the dependent variables P and T. The stellar parameters resulting from this procedure now satisfy the correct energy conservation law. If the time step is chosen properly ΔE_Q is always only a very small fraction of the specific internal energy and thus the new stellar parameters are still rather accurate numerical solutions of the other basic equations. The small deviations that are present are corrected again at the next time step. It should be noted, perhaps, that this method is similar to the usual treatment of the changes of the chemical composition with time in ordinary stellar evolution calculations.

Again following the description by Kippenhahn, Weigert and Hofmeister (1967) the independent variable M_r and the dependent variables P, T, L_r, r, and v were replaced by an equal number of corresponding transformed variables when the difference equations were formulated. Several different versions of the difference equations were tested. While almost no differences in the numerical solutions could be detected, the number of iterations that were needed to reach a given accuracy was found to depend strongly on how the difference equations were formulated. The formulation that was used eventually is given in the Appendix.

As noted before by other authors, the convergence of the Henyey method sometimes depends critically on how well the starting model for the iterations at time $t + \Delta t$ is pre-estimated from the stellar parameters and time derivatives at time t. For hydrostatic stellar evolution calculations often a linear extrapolation with time of all dependent variables is sufficient. An attempt to use such a simple linear extrapolation for the pulsation calculations, however, resulted in rather slow convergence or no convergence at all. Therefore, the extrapolation procedure was modified in the following way: all dependent variables except of the temperature T were extrapolated linearly. Since (possibly with exception of the surface layers) the periodic changes of P and T in a pulsating star are always very nearly adiabatic, the temperature was extrapolated in such a way that the pre-estimated change with time of P and T became adiabatic. Be $T^0_{t+\Delta t}$ the pre-estimated temperature at time $t+\Delta t$ (the superscript 0 indicating that these values of T are not the solution but only the zero order approximation to start the iterations at time $t+\Delta t$) and be $P^0_{t+\Delta t}$ the corresponding linearly extrapolated variable P, then an adiabatic change of P and T at time $t+\Delta t$ means that for any value M_r the variable $T^0_{t+\Delta t}$ satisfies either

$$\ln T^0_{t+\Delta t} - \ln T_t = \nabla_{\text{ad}} (\ln P^0_{t+\Delta t} - \ln P_t) \quad (17)$$

when backward time differences are used or

$$\ln T^0_{t+\Delta t} - \ln T_t = \frac{1}{2} \nabla_{\text{ad}} (\ln P^0_{t+\Delta t} - \ln P_t) + \left(\frac{\partial T}{\partial t}\right)_t \frac{\Delta t}{2} \quad (18)$$

when centered time differences are used (the subscript t means that the values at time t of the subscripted quantities are to be taken). ∇_{ad} is

$$\frac{\partial \ln T}{\partial \ln P}$$

for a strictly adiabatic change of P and T.

Because of Eq. (6) ∇_{ad} can also be expressed by

$$\nabla_{\text{ad}} = \left[\left(4 - \frac{3}{2}\beta\right) + 6\,(1-\beta)\,(4\,\beta^{-1} - 3)^{-1}\right]^{-1} \quad (19)$$

where β is the ratio of gas pressure and total pressure, or

$$\beta = 1 - \frac{a\,T^4}{3\,P}\,. \quad (20)$$

Since ∇_{ad} is a nonlinear algebraic function of T both (17) and (18) are nonlinear equations for $T^0_{t+\Delta t}$, which can be solved, however, easily by the following fast converging iteration procedure: a first approximation for $T^0_{t+\Delta t}$ is derived by extrapolating T linearly with time. From this values a first approximation for $\nabla_{\text{ad},t+\Delta t}$ is calculated from Eq. (19). Using this approximation of ∇_{ad} and either Eq. (18) or Eq. (19) an improved $T^0_{t+\Delta t}$ is derived. These values are used to derive a better ∇_{ad}, and so on. Usually it takes not more than three iterations to satisfy (18) or (19) within the computer accuracy.

With the "adiabatic" extrapolation described above the Henyey method was converging very well, usually requiring between two and five iterations. With the star divided into 138 mass shells, each iteration took about 0.6 seconds on an IBM 360/91 computer. The non-equidistant mass steps ΔM_r were chosen according to the same criteria as used in hydrostatic stellar evolution calculations. With backward time differences usually a time step of 200 seconds was chosen. This corresponds to about 173 time steps per pulsation period. Only at certain phases of the high amplitude pulsations, e.g. when strong shock waves reached the stellar surface, much shorter time steps (down to 20 seconds) and more iterations per time step were necessary.

V. The Initial Value Problem

In principle the most logical way to calculate the main-sequence evolution of a 130 $M_\odot$ star would be to solve numerically the dynamical equations of stellar structure [Eqs. (1) to (4)], using as initial values the parameters of a 130 $M_\odot$ star that is just completing its pre-main-sequence contraction phase. But, if we assume that the initial velocity amplitude is equal to the final pre-main-sequence contraction velocity (about 10 cm s^{-1} at the surface) and if we calculate the amplitude increase with time according to the linear pulsation theory, we can estimate that a 130 $M_\odot$ main-sequence star survives without mass loss for at least 20000 years or more than 10^7 pulsation periods. For accuracy reasons, at least 100 time steps are necessary for each period. Thus, an unworkable amount of computing time would be required by such a straight forward computation. In order to avoid this the following numerical procedure was used: the rate of energy gain of the pulsations was increased artificially by multiplying after each time step the values of the velocity $v(M_r, t)$ by a factor slightly larger than unity. Thus the pulsation amplitude is growing more rapidly than it would when the nuclear reactions were the only source of mechanical energy. There are, however, unwelcome by-effects of such an artificial energizing mechanism: 1) introducing an artificial energizing mechanism is equivalent to solving a set of modified basic equations. This will result in slightly different or distorted solutions; 2) spurious higher harmonics which are not energized by the nuclear reactions may be energized by the artificial mechanism; 3) since the energy law is violated deliberately, a time sequence calculated with such an artificial mechanism does not give direct information on the rate of energy gain (or loss) of the real stellar pulsations.

Test calculations with and without the artificial energizing showed that the distortion by an artificial amplitude increase of 3 per cent per pulsation period is only a few per cent and therefore negligible. A more serious problem is the energizing of spurious harmonics. In a real 130 $M_\odot$ star the overtones are always damped and not energized by the nuclear reactions since the ratio of the pulsation amplitudes in the stellar core (where the mechanical energy is generated) and near the surface (where mechanical energy is transformed into radiation and thus lost) is much smaller for the harmonics than for the fundamental mode. However, since the amplitude decrease of the first harmonic due to the radiation effect is less than 10^{-2} per cent, this effect is not sufficient to suppress spurious overtones if the artificial energizing mechanism with an amplitude increase of 3 per cent per period is used. Therefore, such an artificial energizing mechanism has to be supplemented by an artificial selective damping mechanism which like the radiation effect is more effective on the harmonics than on the fundamental mode. Such an effect was introduced by the use of backward time differences in the difference equations. Backward time differences (for an exact definition see the Appendix) mean that there is a systematic phase shift of $\Delta t/2$ between the arguments of the dependent variables and the arguments of their time derivatives. In the case of the pulsation equations this phase shift results in damped oscillations. (For the basic mathematical properties of such "time-laged" differential equations see e.g. Myschkis, 1955.) Since the phase shift expressed in units of the pulsation periods is larger for the higher modes, the harmonics are damped stronger than the fundamental mode. Thus the use of backward differences indeed has qualitatively the same selective damping effect as the radiative heat transfer in the outer layers of the star. But with a time step of $\Delta t = 200$ seconds the selective damping by backward differences is strong enough to make it possible that the amplitude of the fundamental mode is increased by several per cent without energizing spurious overtones. Another important advantage of backward time differences is the high numerical stability of the resulting difference equations (Richtmyer, 1957). Because of this reason they are used in most hydrodynamic initial value calculations. A disadvantage of backward differences is, for the present problem, that strongly nonlinear pulsations are distorted since the higher order Fourier components of the fundamental mode are more strongly damped than the lower order components. This distortion effect is actually much stronger than that of the artificial energizing mechanism itself. In order to determine this distortion parts of the time sequence calculated with the artificial energizing mechanism and backward differences were repeated with centered time differences and without artificial energizing. Since the results of these calculations were energetically correct solutions, they were also used to derive the true values of the gain of mechanical energy and the amplitude increase as a function of the pulsation amplitude. For this purpose the mechanical energy W gained or lost during one pulsation period was calculated by means of the mechanical work integral

$$W = \int_{t_0}^{t_0+\Pi} \int_0^M P \frac{\partial V}{\partial t} \, dM_r \, dt \,. \tag{21}$$

Here Π is the pulsation period. Because of numerical reasons, which are described below, W was not actually calculated by direct integration but derived by a numerically more accurate indirect method.

VI. The Mechanical Work Integral

In a pulsating 130 $M_\odot$ main-sequence star the gain of pulsation energy during one pulsation period is always only a small fraction (in the order of 10^{-6}) of the total pulsation energy. The pulsation is therefore very nearly adiabatic. In such a case much more accurate numerical results are obtained if the work integral [Eq. (21)] is not evaluated by direct integration but by the following indirect method:

the pressure $P(M_r, t)$ in the pulsating star can be written as

$$P(M_r, t) = P_0(M_r, t) + P_1(M_r, t) \tag{22}$$

where $P_0(M_r, t)$ is defined as the pressure that would be observed in the star during a hypothetical periodic change of volume with the specific volume $V(M_r, t)$ as a function of time being exactly like the one observed in the real pulsating star, but where at any time and at any mass shell the condition

$$\frac{\partial L_r}{\partial M_r} = \varepsilon_N \tag{23}$$

is fulfilled. The condition obviously means that the change of volume is exactly adiabatic. Since in the presence of viscosity no adiabatic and strictly periodic function P_0 can be defined (because the internal energy would increase with time), it will be assumed for the following that no shock waves and thus no artificial viscosity are present.

Using the above definition of P_0, the work integral Eq. (21) becomes

$$W = \int_{t_0}^{t_0+\Pi} \int_0^M \left(P_0 \frac{\partial V}{\partial t} + P_1 \frac{\partial V}{\partial t}\right) dM_r \, dt \,. \tag{24}$$

Since no mechanical energy is lost or gained in a periodic adiabatic process, we have

$$\int_{t_0}^{t_0+\Pi} \int_0^M P_0 \frac{\partial V}{\partial t} dM_r\, dt = 0\,. \tag{25}$$

Thus Eq. (24) becomes

$$W = \int_{t_0}^{t_0+\Pi} \int_0^M P_1 \frac{\partial V}{\partial t} dM_r\, dt\,. \tag{26}$$

Since the star pulsates very nearly adiabatic, in most layers of the star, P_1 is always much smaller then P. Therefore, in order to calculate W within given accuracy limits, a smaller relative accuracy is needed for P_1 if Eq. (26) is used than is necessary for P if Eq. (22) is used. In order to derive an expression for P_1, we define U_1 and β_1 by the two equations

$$U(M_r, t) = U_0(M_r, t) + U_1(M_r, t)\,, \tag{27}$$

$$\beta(M_r, t) = \beta_0(M_r, t) + \beta_1(M_r, t)\,, \tag{28}$$

where U_0 and β_0 are defined as the specific internal energy and the ratio of gas and total pressure, which would be observed together with P_0 in the hypothetical adiabatic change of volume. With these definitions, the energy balance equation for the pulsating star [Eq. (2)] becomes

$$\varepsilon_N - \frac{\partial L_r}{\partial M_r} - \frac{\partial U_0}{\partial t} - \frac{\partial U_1}{\partial t} - P_0 \frac{\partial V}{\partial t} - P_1 \frac{\partial V}{\partial t} = 0\,. \tag{29}$$

The same equation for the hypothetical adiabatic change of volume reads

$$-\frac{\partial U_0}{\partial t} - P_0 \frac{\partial V}{\partial t} = 0\,. \tag{30}$$

Equations (29) and (30) combined give

$$\frac{\partial U_1}{\partial t} = \varepsilon_N - \frac{\partial L_r}{\partial M_r} - P_1 \frac{\partial V}{\partial t} \tag{31}$$

or

$$U_1(M_r, t) = \int_{t_0}^{t} \left(\varepsilon_N - \frac{\partial L_r}{\partial M_r}\right) dt - \int_{t_0}^{t} P_1 \frac{\partial V}{\partial t} dt + U_1(M_r, t_0)\,. \tag{32}$$

Another relation for U_1 is derived from Eqs. (5), (6) and (20):

$$U = U_0 + U_1 = (P_0 + P_1)\left(3 - \frac{3}{2}\beta\right) V \tag{33}$$

or since

$$U_0 = P_0 V \left(3 - \frac{3}{2}\beta_0\right) \tag{34}$$

we also have

$$U_1 = U - U_0 = V P_1 \left(3 - \frac{3}{2}\beta\right) - \frac{3}{2} V P_0 \beta_1\,. \tag{35}$$

Since the pulsation is nearly adiabatic, we have $\beta_1 < \beta$. Thus, because of the definition of β [Eq. (20)] β_1 becomes with good approximation

$$\beta_1 = \frac{P_1}{P_0}(\delta^{-1} - \beta) \tag{36}$$

where

$$\delta = 4\beta^{-1} - 3\,. \tag{37}$$

From Eqs. (35) and (36) we obtain

$$U_1 = 3 P_1 V (1 - (2\delta)^{-1}) \tag{38}$$

and finally by combining the Eqs. (38) and (32)

$$3 P_1 V \left(1 - (2\delta)^{-1}\right) = \int_{t_0}^{t} \left(\varepsilon_N - \frac{\partial L_r}{\partial M_r}\right) dt - \int_{t_0}^{t} P_1 \frac{\partial V}{\partial t} dt + U_1(M_r, t_0)\,. \tag{39}$$

Provided, $U_1(M_r, t_0)$ is known, $P_1(M_r, t)$ can now be calculated easily by solving numerically the integral Eq. (39) for discrete values of M_r. In order to simplify the calculations, the constant t_0 was always chosen to correspond approximately to the phase of maximum contraction, where $U_1(M_r, t)$ is zero. Although in nonlinear pulsations the values of $U_1(M_r, t)$ for different M_r do not quite simultaneously change their sign, always $U(M_r, t_0) = 0$ was assumed. From Eqs. (26) and (39) follows that the error that is introduced in W by this inaccuracy is in the order of

$$\Delta W \sim \int_0^M \frac{1}{3} U_1(M_r, t_0) \int_{t_0}^{t_0+\Pi} \cdot (1 - (2\delta)^{-1})^{-1} V^{-1} \frac{\partial V}{\partial t} dt\, dM_r\,. \tag{40}$$

If δ is independent of time (like in an ideal gas without radiation pressure), the time integral in Eq. (40) can be evaluated analytically and is always equal to zero. In the general case at least the order of magnitude of ΔW can be determined numerically if $U_1(M_r, t_0)$ is known approximately. In this way ΔW was always found to be much less than 1 per cent of W and thus negligible.

In principle, W could also be calculated in a much simpler way from the formula

$$W = \int_0^M \int_{t_0}^{t_0+\Pi} \left(\varepsilon_N - \frac{\partial L_r}{\partial M_r}\right) dt\, dM_r \tag{41}$$

which follows from Eqs. (39) and (26), since for a strictly periodic pulsation we have

$$U_1(M_r, t_0) = U_1(M_r, t_0 + \Pi) . \tag{42}$$

But numerically Eq. (41) is hardly more accurate than a direct integration in Eq. (21) since this formula is very sensitive to small deviations from periodicity in the numerical solutions of the pulsation equations. There are three sources for such deviations from periodicity: 1) in a vibrationally unstable star the pulsations cannot be exactly periodic, since the amplitude is increasing slowly. 2) the truncation errors at each time step tend to accumulate with time and thus to introduce additional spurious deviations from strictly periodic solutions; 3) as noted before, the mean values of the dependent variables, averaged over one pulsation period, depend slightly on the pulsation amplitude. Especially when the artificial energizing mechanism is used, the amplitude increase is too fast to leave time for a complete thermal adjustment of these mean stellar parameters. This results in a slow nonperiodic drift of $U(M_r, t)$. If W is calculated according to Eq. (41) such a drift may produce erroneous results. E.g. with a pulsation amplitude of $\delta R/R = 5 \times 10^{-4}$ and with a spurious drift of the temperature in the stellar core of 2° K per pulsation period, W derived from Eq. (41) will be wrong by about a factor of 10. If Eqs. (26) and (39) are used, the error will be less than one tenth of a per cent. Thus Eq. (41) cannot be used to derive W accurately. But, since the integrand in Eq. (41) is part of Eq. (39), a comparison of the inaccurate value of W derived from Eq. (41) with the "correct" value derived from Eqs. (26) and (39) can be used to estimate the accuracy of the more accurate second value of W. By this method the error of W was found to be not larger than 4 per cent.

As stated above, the definitions of P_0 and P_1 and Eq. (26) are not compatible with the presence of an artificial viscosity. Therefore, at large amplitudes the star was divided into an inner region (containing about 99.99 per cent of the stellar mass) where no shock waves occurred and where no artificial viscosity was used, and an outer region where the shock waves occurred and where consequently a $Q \neq 0$ had to be used. Then the work integral W_I for the inner region alone was calculated using the indirect method described above. In addition the mechanical energy W_0 transferred by the inner region to the outer region during one pulsation period was calculated from

$$W_0 = \int_{t_0}^{t_0+\Pi} P_B(t) \frac{d\tilde{V}_I(t)}{dt} dt \tag{43}$$

where $\tilde{V}_I(t)$ is the volume of the inner region, or

$$\tilde{V}_I(t) = \int_0^{M_B} V(M_r, t)\, dM_r \tag{44}$$

P_B is the pressure at the boundary between the inner and the outer region and M_B is the mass of the inner region. The difference $W_I - W_0$ is obviously the net amount of mechanical energy that is actually gained by the interior region during one pulsation period. Because such a small fraction of the stellar mass is contained in the outer region, the mechanical energy gained by the interior region is with good approximation equal to the mechanical energy gained by the star. Thus we have with good approximation

$$W = W_I - W_0 . \tag{45}$$

In principle, the numerical evaluation of Eq. (43) involves the same difficulties as a direct integration of the work integral in Eq. (21). However, since the pressure P_B at $M_r = M_B$ is smaller by several orders of magnitude than the mean pressure in the interior region, W_0 can be calculated with about the same absolute accuracy by direct integration as W_I by the indirect method.

Although even near the center of the star the solutions eventually deviate considerably from the solutions of the linear theory, the relative amplitude increase with time stays with good approximation independent of M_r throughout the interior region of the star. Therefore, like in the linear theory the pulsation amplitude $A(M_r, t)$ in the interior region as a function of time can be expressed by

$$A(M_r, t) = A_0(M_r) \exp(Kt) . \tag{46}$$

In contrast to the linear theory (Schwarzschild and Härm, 1959), at large amplitudes, K is not independent of time. But at a given amplitude K can still be calculated with good approximation from the formula

$$K = \frac{1}{2} \frac{W}{E_P \Pi} \tag{47}$$

where E_P is the total pulsation energy. (Strictly speaking, E_P is, of course, the energy of the pulsation

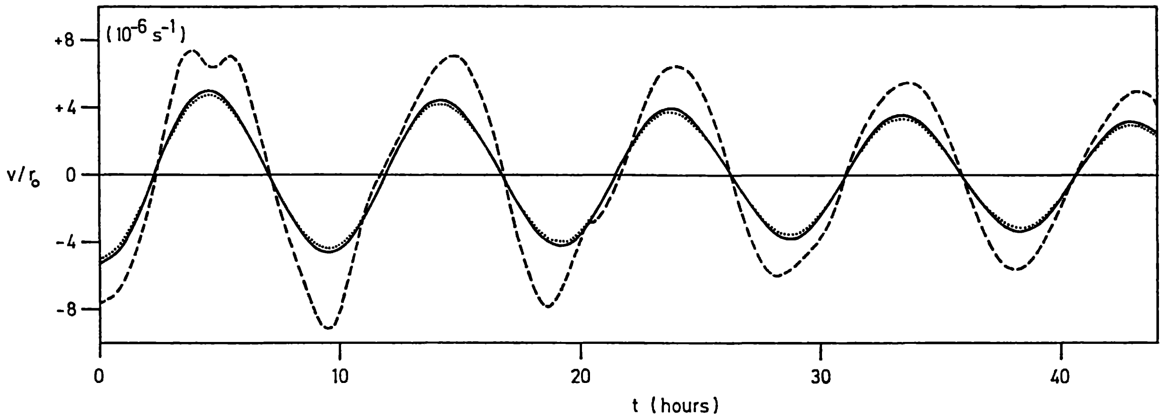

Fig. 1. The normalized velocity $v_r(M_r, t)/r_0(M_r)$ for three layers of a pulsating 130 $M_\odot$ main-sequence star. The three layers are: the surface ($r_0 = 1.03 \times 10^7$ km, broken line), $M_r = 0.50\, M$ ($r_0 = 3.69 \times 10^6$ km, solid line), and $M_r = 0.01\, M$, ($r_0 = 7.89 \times 10^5$ km, dotted line). The pulsations shown in this figure were started with initial values taken from the linear pulsation theory (see text). The damping is due to the use of backward time differences

of the interior region. But since the outer region contains less than 1 per cent of the total pulsation energy, E_P is also with good approximation the total pulsation energy.)

VII. Numerical Results and Discussion

If, as suggested above, the initial velocity amplitude is about equal to the final pre-main-sequence contraction velocity, the linear adiabatic pulsation theory used by Schwarzschild and Härm is at the beginning a very good approximation. Pulsations of small amplitude were therefore only computed in order to test the computer program. At an amplitude corresponding to a relative radius variation of $\delta R/R = 5 \times 10^{-4}$ the solutions of the nonlinear and nonadiabatic equations and the results of the linear adiabatic theory were found to be identical within the computational accuracy of the linear calculations. Significant deviations from the results of the linear theory have to be expected if either the condition $\delta R/R \ll 1$ is violated or if somewhere in the star the velocity $v\ (M_r, t)$ surpasses the velocity of sound. From the hydrostatic stellar model and from the linear theory it can be estimated that the velocity amplitude in the photosphere reaches the local sound velocity already at a pulsation amplitude corresponding to $\delta R/R = 0.09$. The nonlinear calculations were therefore started at approximately this amplitude. The initial values were taken from the results of the linear theory. Since $\delta R/R$ is already too large to obtain accurate initial values for the fundamental mode of the nonlinear solutions from the linear theory, no attempt was made to derive the linear solutions very accurately. In order to eliminate spurious higher harmonics that are possibly introduced by the inaccurate initial values, the calculations were started with backward time differences but, at first, without artificial energizing. The results are shown in Fig. 1. There the velocity $v\ (M_r, t)$ divided by the corresponding radius of the hydrostatic model $r_0\,(M_r)$ is plotted against the time t for three stellar layers: for the visible surface ($\tau = 2/3$, $r_0 = 1.03 \times 10^7$ km, broken line), for a mass shell in the deep interior ($M_r = 0.5\ M$, $r_0 = 3.69 \times 10^6$ km, solid line), and for a mass shell near the stellar center ($M_r = 0.01\ M$, $r_0 = 7.89 \times 10^5$ km, dotted line). In good agreement with the linear theory the normalized velocity v/r_0 changes only little between $M_r = 0.01\ M$ and $M_r = 0.5\ M$. In both these layers the velocity curve is approximately a (phase shifted) sinus curve with exponentially decreasing amplitude, which is characteristic for a damped linear pulsation. The damping, of course, is due to the backward time differences. The pulsation period is 0.400 days which still agrees within 1 per cent with the fundamental pulsation period derived from the linear theory. The double peak at the first maximum of the surface velocity curve indicates that, due to the numerical inaccuracies, overtone components were present in the initial values. But as shown by Fig. 1 the overtones are damped out by the backward time differences within a few pulsation periods. With only the fundamental mode still present, the velocity curve becomes sinosoidal in all layers of the star. The decrease of the velocity amplitude from the surface to the center and the rate of amplitude increase

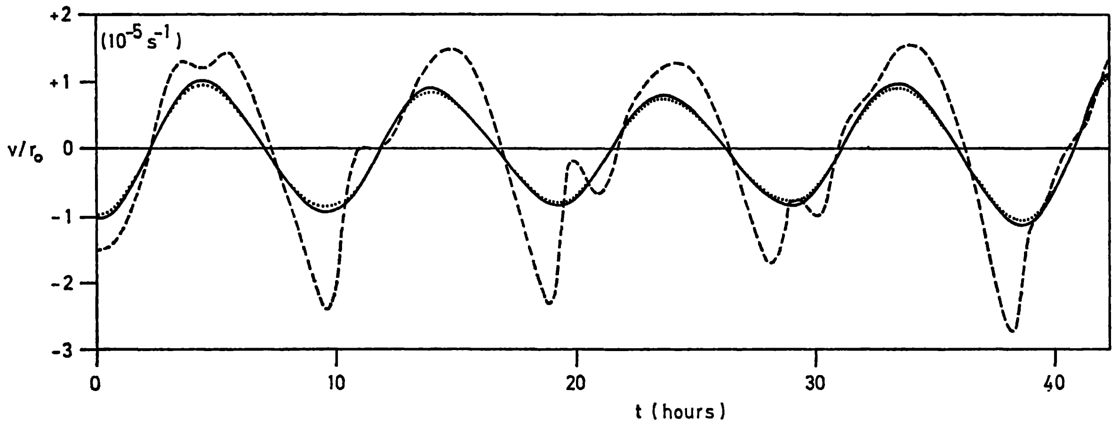

Fig. 2. Normalized velocity for three layers of a pulsating 130 $M_\odot$ main-sequence star. The three layers are the same as in Fig. 1. Compared to Fig. 1, the initial velocity amplitude is twice as large. Nonlinear effects make the difference to Fig. 1

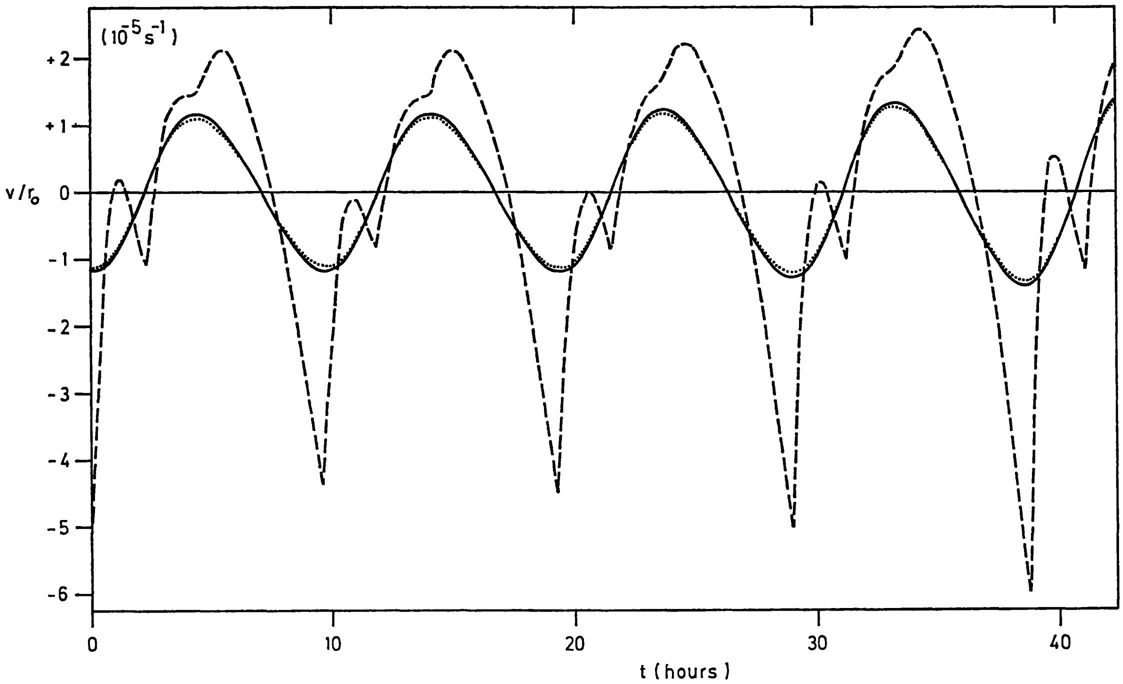

Fig. 3. Normalized velocity for three layers of a pulsating 130 $M_\odot$ main-sequence star. The three layers are the same as in Figs. 1 and 2. The pulsation amplitude is about 20 per cent larger than the initial amplitude of Fig. 2. The nonlinear effects have become much stronger therefore

derived from the work integral still agree within a few per cent with the values predicted from the linear theory. Thus the initial pulsation amplitude in Fig. 1 turned out to be still too small to get marked deviations from the linear theory. These calculations were therefore repeated with the initial pulsation amplitude twice as large. The results are shown in Fig. 2. Although the velocity curves of the two interior mass shells deviate now somewhat more from damped sinus curves, the deviations are still only small fractions of the velocity amplitude in these layers. At the surface, however, the deviations have increased strongly. The most striking feature of the surface velocity curve at this amplitude

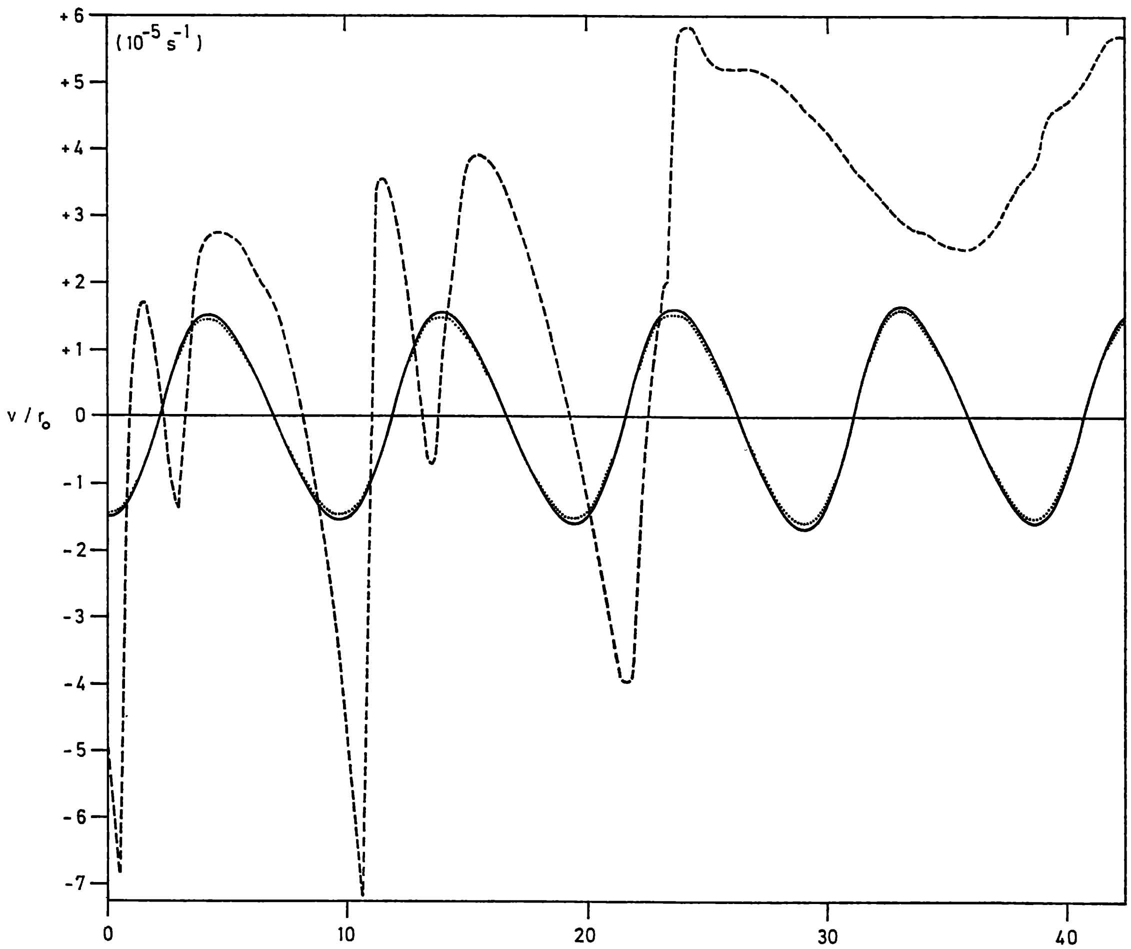

Fig. 4. The normalized velocity for three layers of a pulsating 130 $M_\odot$ main-sequence star. The three layers are the same as in Fig. 1. At this amplitude the positive and negative surface velocities do no longer cancel out when averaged over one pulsation period, but now the average is always positive. After $t = 23$ hours (in Fig. 4) even the surface velocity itself stays positive. Thus, at this amplitude an expanding shell around the star is formed

is the strong deceleration which occurs after the phase of maximum negative velocity. Actually this sudden deceleration is an outward acceleration of the surface layers caused by the passage of a shock wave through the stellar surface. [The details of the acceleration of stellar surface layers by shock waves will not be described here, since extensive descriptions of this mechanism have been given by other authors. See e.g. Hazlehurst (1962), Kushwaha and Odgers (1960), Sparks (1969).] The shock wave develops during the contraction phase just below the photosphere and then travels to the surface. Since the occurrence of the shock wave is a truely nonlinear feature of the fundamental mode at this amplitude, it cannot be eliminated by the backward differences. The apparent decrease with time of the strength of this effect in Fig. 2 is due to the slowly decreasing pulsation amplitude and the very strong amplitude dependence of the shock strength. The effect increases again, when the amplitude is increased artificially, as demonstrated in the last pulsation period of Fig. 2.

In order to find out how the properties of the fundamental mode change with increasing amplitude, the nonlinear calculations were continued for about 20 pulsation periods while the interior pulsation amplitude was increased artificially at a rate of about 3 per cent per period. The velocity curves at two later stages of this time sequence are shown in Fig. 3 and Fig. 4. The zero points of the time axis of these figures are arbitrary. In Fig. 3 the pulsation amplitudes of the interior mass shells are only about 20 per cent larger than the initial amplitude in Fig. 2.

The total variation of the surface velocity, however, has almost doubled, since periodically recurring shock waves now transport additional mechanical energy to the surface layers. The sudden sign-reversal of the acceleration at the phase of maximum negative velocity also became much more pronounced, since the strength of the shock front which causes this reversal is growing rapidly with increasing pulsation amplitude. Although the shock waves originate now in somewhat deeper layers than at the pulsation amplitude of Fig. 2, they are still confined to the outermost layers of the star. This is demonstrated best by Fig. 5 where the radius $r\,(M_r, t)$ is plotted against the time t for several selected values of M_r. The velocity amplitude corresponding to Fig. 5 is slightly larger than the maximum amplitude in Fig. 3. But the values for Fig. 5 were not taken from the time sequence of Figs. 1 to 4 but from the more accurate calculations with centered time differences. As shown by Fig. 5 the strong deviations from the linear solutions due to the recurring shock waves are present only in a thin surface layer, containing about 10^{-3} per cent of the stellar mass and (at this amplitude) only about 5 per cent of the stellar radius.

When the amplitude is increased further, at first the shape of the surface velocity curve stays essentially constant. But the surface radius curve becomes more and more nonperiodic, since the effective displacement of the stellar surface during one pulsation period, given by

$$d = \int_{t_0}^{t_0+\Pi} v(M_r, t)\,dt \tag{48}$$

is not longer zero like in a truely periodic radius change. Instead we obtain $d > 0$, which means that the mean radius of the star is increasing. This stage of the dynamical evolution is illustrated by Fig. 4. Here positive (or outward) velocities become more and more dominant until eventually $v(M_r, t)$ stays continuously positive. At this final stage the star consists now of a periodically pulsating interior and a continuously expanding shell. This shell is supported mainly not by gas or radiation pressure but by the periodic transfer of momentum by the recurring shock waves. As soon as the shell is formed, the total variation of the surface velocity does no longer increase, but now starts to decrease (as shown on the right hand side of Fig. 4). This happens because the shock waves now loose so much energy while travelling through the expanded and further expanding outermost layers of the star, that they cannot longer overtake or reach the supersonically expanding surface. In addition the velocity curve is smoothed out since any deceleration of the outward moving layers just below the surface results in a decrease of the effective gravitational acceleration

$$g_{\text{eff}} = \frac{GM_r}{r^2} + \frac{\partial^2 r}{\partial t^2} \tag{49}$$

and thus in an expansion of these layers. A free falling shell e.g. would simply be blown appart by the strong radiation pressure gradient near the surface.

From calculations of the work integral W it was found that the radiative damping of the pulsations increases strongly when the shell is formed, and that W becomes negative when the amplitude is increased further. Therefore, the artificial energizing mechnism was turned off at the amplitude of Fig. 4 and a few more periods were calculated without the artificial amplitude increase. Although during these periods the expansion velocity at the surface stayed essentially constant (at about 500 km s^{-1}), the velocity eventually reached the escape velocity since with continuously increasing radius the escape velocity became smaller. Matter that is moving faster than the escape velocity is permanently lost from the star, since it can never fall back on its surface. Thus the star starts to lose mass shortly after the shell is formed. At this stage the calculations were stopped, since with the rapidly increasing radius and the decreasing surface temperature the surface boundary conditions and the assumptions on $\varkappa$ become too wrong to get meaningful results from the model calculations.

Since, for numerical reasons, artificial effects (artificial viscosity, artificial energizing, and artificial selective damping by the backward differences) were included, the model calculations described above need not be characteristic for the behaviour of a real star. However, additional calculations without the artificial energizing, with centered time differences, and with several different values of the viscosity constant l in Eq. (14), showed that qualitatively the results are independent of the artificial effects. Quantitatively at large amplitudes the ratio of the surface velocity amplitude and the interior velocity amplitude (but not as much the shape of the velocity curve) was found to be strongly affected by the backward time differences and the artificial viscosity. While this effect is still negligible for the amplitude of Fig. 2 the interior velocity amplitude in Fig. 4 is too large compared to the surface amplitude by a fac-

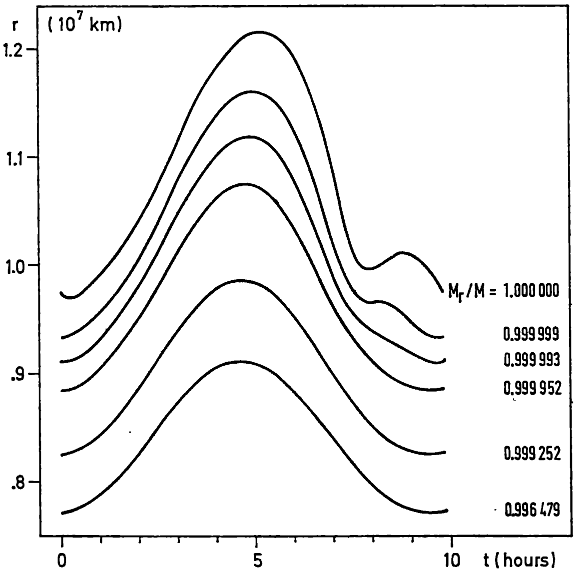

Fig. 5. The radius function $r(M_r, t)$ near the surface just before the shell is formed

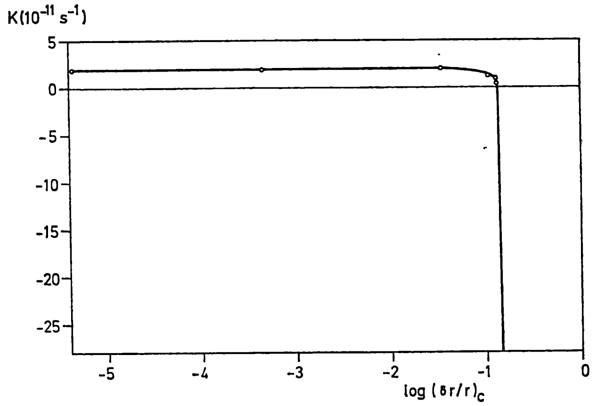

Fig. 6. The exponent of amplitude increase as a function of the interior pulsation amplitude for a 130 $M_\odot$ zero-age-main-sequence star

tor of 1.3 ± 0.1. The numerical uncertainty of this factor results from a possibly rather inaccurate extrapolation to zero artificial viscosity, which is necessary since, unlike the backward time differences and the artificial energizing, the artificial viscosity cannot be eliminated completely from the calculations. The computations with the centered time differences also showed that the star forms its shell and starts to loose mass at an interior pulsation amplitude about 30 per cent smaller than in Fig. 4. But in spite of the strong dependence of the surface velocity on the artificial viscosity, the work integral was found to depend not as much on the viscosity. This is apparently due to the fact that only in the outermost layers, where the optical depth is in the order of unity, the energy loss is strongly affected by the artificial viscosity. The contribution of these layers to the total loss of mechanical energy is not very large, however, since the pressure is already very small there.

The relative gain of mechanical energy as a function of the pulsation amplitude is given by Fig. 6. Here K, as defined by Eq. (47), is plotted against the relative radius variation $\delta r/r_0$ near the center of the star. In order to derive the leftmost point for Fig. 6 another time sequence was computed, in which the interior pulsation amplitude was increased to a value about 20 per cent above the value where the shell was formed. At this amplitude the loss of mechanical energy during one pulsation period was found to be at least two orders of magnitude larger than the gain of mechanical energy in the core. (The corresponding point, therefore, is far outside the lower margin of Fig. 6.) The main reason for this extremely strong damping is that the shock waves become so strong that a relatively large portion of the shell (containing up to $10^{-5}\,M_\odot$) is ejected during each pulsation period. This very strong increase of the damping confirms that the pulsation amplitude can certainly not increase to a value substantially above the amplitude where the expanding shell is formed. Since the gain of mechanical energy in the core is approximately proportional to the square of the pulsation amplitude, the upper limit for the pulsation amplitude also means that there is an upper limit for the energy gain per pulsation period. And since the kinetic energy of the matter that is accelerated to the escape velocity during one pulsation period cannot be larger (in a quasi-stationary state) than the mechanical energy gained in this time interval, the limiting pulsation amplitude also means an upper limit for the mass loss rate. In particular, the mass δM ejected during one pulsation period cannot be larger than

$$\delta M_{\max} = \frac{2}{v_e^2} W_I \tag{50}$$

where v_e is the escape velocity and W_I is the net gain of mechanical energy of the stellar interior below the layers that are ejected. Using Eq. (50) and the work integral an upper limit of

$$\delta M = 4 \times 10^{-5}\,M_\odot$$

per year for the 130 $M_\odot$ star on the zero-age-main-sequence was found. This mass loss rate agrees approximately with the amount of mass that was found to be eventually streaming from the star in the numerical solutions. But since probably not enough pulsation periods could be calculated for the shell stage of the star in order to get a real quasi-stationary state the estimate from Eq. (50) seems more reliable. Because of the same reason the effective radius R_e (the radius of $\tau = 2/3$) after the expanding shell is formed also cannot be determined accurately from the model calculations. But from the condition that at R_e the growth of τ due to the outstreaming mass and the decrease of τ due to the expansion of the atmosphere above R_e must compensate, R_e can be estimated to be roughly 4 times the initial stellar radius (or about 60 $R_\odot$). Because of Eq. (8) and since the bolometric luminosity changes only slightly, the effective temperature of the star decreases proportional to $R_e^{-1/2}$ when the shell is formed. Thus with $R_e = 60\,R_\odot$ the effective temperature of the star becomes about 28 500 °K.

Since the limiting pulsation amplitude in the interior and thus the maximum possible mass loss rate of the star is much smaller than predicted from the linear theory, the main result of the nonlinear calculations is that a vibrationally unstable 130 $M_\odot$ main-sequence star can survive much longer than assumed so far. With the mass loss rate derived above, the star can exist for more than 10^6 years (or nearly its total main-sequence live time as determined by the exhaustion of hydrogen in the core) before becoming vibrationally stable again due to the decrease of its mass. However because of the change of the chemical composition and the resulting change of the stellar structure, δM will certainly not be constant over such a long time interval. No nonlinear pulsation calculations were carried out for evolved 130 $M_\odot$ main-sequence stars. However, from hydrostatic model calculations of very massive stars (Stothers, 1966) and from the linear pulsation theory it is known that both, the vibrational instability and the velocity of sound in the outer layers of the star are decreasing with increasing age on the main-sequence, until the star becomes vibrationally stable again after about 1.5×10^6 years (Schwarzschild and Härm, 1959). It seems rather safe, therefore, to predict that the rate of mechanical mass loss is also decreasing with increasing age on the main-sequence. If we assume the mean rate of mass loss to be one half the upper limit derived above, and if we assume further that

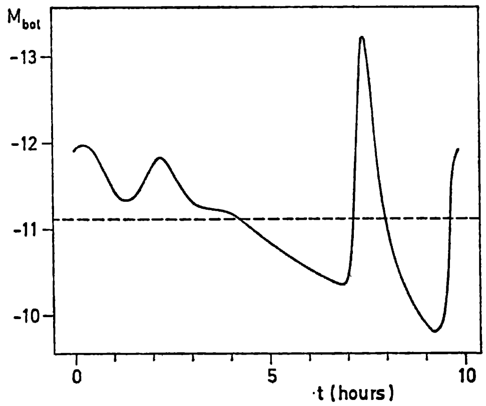

Fig. 7. The bolometric light curve of a pulsating 130 $M_\odot$ main-sequence star at maximum luminosity amplitude (at the beginning of shell formation). The broken line indicates the luminosity of the hydrostatic stellar model

the mass loss continues for 1.5×10^6 years, until the star becomes stable again, actually only about 30 $M_\odot$ or 23 per cent of the original stellar mass are lost on the main-sequence.

Using Eq. (46) and the values of K plotted in Fig. 6, the age corresponding to a given pulsation amplitude can be computed. With the time scale determined by this method, the numerical results described above can be summarized as follows: during the first 18000 years on the main-sequence a 130 $M_\odot$ star looks like a very hot and luminous O star, having the same observable properties as a hydrostatic star of this mass and thus the properties listed in the Table. During this time the star is already pulsating, but the luminosity amplitude is less than 0.01 magnitudes and thus not detectable. For about the next 5000 years the star is a regular variable with rapidly increasing luminosity amplitude and changing light curve. (The computed light curve at maximum luminosity amplitude is shown in Fig. 7.) Then, about 23000 years after the start of the oscillations, the star becomes a P Cyg like object with an effective temperature in the order of 28000°K and a supersonically expanding shell. This evolutionary stage lasts for most of the star's remaining main-sequence live time. During this time the star continuously looses mass, but the total mass loss on the main-sequence will be only a minor fraction of the initial stellar mass.

VIII. Comparison with Observations

Because of the well determined pulsation period and the unique velocity and light curve, obviously the "regular variable" stage of the evolution of a 130 $M_\odot$ main-sequence star would be suited best to identify such a star from observations. However, a comparison of the length of the different phases of the main-sequence evolution shows that only the "P Cyg-stage" lasts long enough to make its observation likely. Since some of the known P Cyg stars belong to the most luminous early type stars in our galaxy, it has frequently been suggested that at least some of these stars are very massive main-sequence stars and that the observed expanding shells and strong mass loss are caused by the vibrational instability. The most thoroughly investigated P Cyg star is the star P Cyg itself. [A detailed review of all observed properties of this star has been given by Beals (1951) and more recently by de Groot (1969).] According to Kopylow (1958) the absolute visual magnitude of P Cyg is $M_v = -8.4$. Thus, if the bolometric correction of a normal B0Ia supergiant is applicable for this peculiar star, its bolometric magnitude is about $M_{\text{bol}} = -11.4$. Luud (1967) already pointed out that this luminosity is much higher than that of any normal supergiant of corresponding spectral class, but approximately equal to the luminosity of a main-sequence star with $M > 100\, M_\odot$. Indeed, a comparison with the Table shows that the bolometric brightness of P Cyg agrees approximately with the luminosity of our 130 $M_\odot$ zero-age-main-sequence star (which is $M_{\text{bol}} = -11.1$). The surface temperature (~ 25000 °K) and radius ($\sim 64\, R_\odot$) of P Cyg as derived by Luud (1967) also agree approximately with those found from the model calculation for the visible surface of the shell of a 130 $M_\odot$ star. The mass loss rates which have been derived from spectral observations of P Cyg by Hutchings (1969) and de Groot (1969) are somewhat larger than those found for the maximum mass of the 130 $M_\odot$ star. According to Hutchings the rate of mass loss of P Cyg is $\delta M = 5 \times 10^{-4}\, M_\odot$ per year, according to de Groot, it is $\delta M = 2 \times 10^{-4} M_\odot$ per year. The 130 $M_\odot$ model calculations resulted in a maximum rate of about $\delta M = 4 \times 10^{-5}\, M_\odot$ per year. But since both, the value derived from the model calculations and the values determined from spectroscopic observations of P Cyg are hardly more than order of magnitude estimates, they are still in agreement within their error limits. Thus, the basic physical properties of P Cyg as they are observed presently are indeed at least compatible with the hypothesis that this star is a main-sequence star of about 130 $M_\odot$. However, it must be noted that at least the visual brightness of P Cyg (and probably the effective temperature and mass loss rate as well) has changed considerably in historical times, as described e.g. by Müller and Hartwig (1920). P Cyg was discovered on August 18, 1600 as a star of about third magnitude. Since the star has never been observed before, its apparent visual magnitude prior to 1600 must have been fainter than $m_v = 6.0$. Between 1600 and 1715 the visual brightness of P Cyg seems to have varied irregularly between $m_v = 3$ and $m_v = 6$. After 1715 the amplitude of the brightness fluctuations decreased and the star reached its present visual brightness of approximately $m_v = 5.0$. If P Cyg is indeed a vibrationally unstable main-sequence star, a sudden increase by several magnitudes of the visual brightness seems not an unlikely event. In contrary, at the evolutionary stage, when the expanding shell is formed, the effective temperature decreases strongly, thereby shifting the energy maximum of the stellar radiation towards the visual region of the spectrum. Since, when the shell is formed, the bolometric luminosity changes only little, the shift of the energy maximum means that the visual brightness is increasing strongly. The numerical calculations carried out with the artificial energizing mechanism are too crude to decide if the relatively strong irregular brightness changes of P Cyg that seem to have occurred between 1600 and 1715 can be explained by the thermal and dynamical adjustment of the outermost stellar layers during the time of shell formation of a vibrationally unstable main-sequence star. The relatively quiet period of P Cyg between 1715 and today, on the other hand, fits rather well to the quasi-stationary state of slow mass loss and small brightness and velocity fluctuations which in the model calculations followed the forming of the expanding shell. In the calculations the periodicity of the pulsations in the deeper layers could no longer be detected in the fluctuations of the brightness and radial velocity at the surface. This may have been due, however, to the fact that the computations were stopped before a real stationary state was reached. Since it takes several pulsation periods for a pressure wave to travel through the expanding shell, even small nonperiodic changes of the sound velocity in the shell tend to destroy any periodicity in the fluctuations of the surface parameters. But because of the continuous mass loss the outer layers of the star will never be exactly in thermal equilibrium. Theoretically at least it seems possible, therefore, that the fluctuations at the surface will stay nonperiodic as long as the shell exists.

While little is known on the short period (<1 day) radial velocity fluctuations of P Cyg, extensive observations of the brightness fluctuations have been carried out by Magalashvili and Kharadse (1967a, b). From observations that covered the time between 1951 and 1960 these authors found superposed on the irregular light variations indeed a regular variation of about 0.1 magnitudes with a period of 0.500656 days. Because of the shape of the light curve Magalashvili and Kharadse suggested that P Cyg is a W UMa like binary system with an orbital period of one half day. But Fernie (1968) showed that this hypothesis is incompatible with the spectroscopic observations. The 0.500 day period observed by Magalashvili and Kharadse is significantly longer than the 0.403 day period of the pulsating interior of the 130 $M_\odot$ star after the shell is formed. But 0.5 days are about equal to the initial pulsation period of a 170 $M_\odot$ star. (A mass of 170 $M_\odot$ also seems to fit even better to the observed luminosity of P Cyg.) All other attempts to explain the regular component of the brightness fluctuations reported by Magalashvili and Kharadse lead to serious contradictions (de Groot, 1969). Thus, these observations may indeed be the most direct evidence that P Cyg is a vibrationally unstable main-sequence star with a mass larger than 100 $M_\odot$. This, in turn, would confirm the result of the nonlinear pulsation calculations that stars with masses in the order of 130 $M_\odot$ are not destroyed by their vibrational instability when they reach the main-sequence, but that they become P Cyg like objects and survive without losing much of their total mass until they become stable again towards the end of their main-sequence evolution.

The writer wishes to thank Dr. R. Kippenhahn for his interest in this work, for helpful suggestions, and for making his computer program available for the hydrostatic calculations. The writer also thanks Dr. Fricke and all the colleagues at Göttingen for helpful and interesting discussions. The numerical calculations were carried out on the IBM 7040 computer of the Aerodynamische Versuchsanstalt at Göttingen and at the computer facilities of the Max-Planck-Institut für Physik und Astrophysik at Munich. I am very grateful to all my colleagues at Munich for their hospitality and assistance.

Appendix

The Difference Equations

In the difference equations in place of the independent variable M_r and the dependent variables P, T, r, L_r, and v the transformed variables

$$\xi = \ln\left(1 - \frac{M_r}{\eta M}\right) \qquad (\eta = 1.0001)\,, \tag{A 1}$$

$$\Psi = \ln P\,, \tag{A 2}$$

$$\Theta = \ln T\,, \tag{A 3}$$

$$\Xi = \ln r\,, \tag{A 4}$$

$$\Lambda = \ln\left(1 + \frac{L_r}{L'}\right) \qquad (L' = \text{const.} > 0)\,, \tag{A 5}$$

$$\Phi = \frac{v}{r} \tag{A 6}$$

were used. Except of Φ, these transformed variables are identical with those suggested for stellar evolution calculations by Kippenhahn, Hofmeister and Weigert (1967). Using these definitions for each shell between ξ and $\xi + \Delta\xi$ the differential Eqs. (13), (2), (3), (4) and (12) were replaced by the following five difference equations:

$$\begin{aligned} \frac{\Psi_{\xi+\Delta\xi} - \Psi_\xi}{\Delta\xi} &- \frac{G\eta^2 M^2}{4\pi}\big(1 - \exp(\xi)\big)\exp(\xi - 4\,\Xi - \Psi) \\ &- \frac{\eta M}{4\pi}\,(D_{\Phi,t} + \Phi^2)\exp(\xi - \Xi - \Psi) \\ &+ \frac{Q_{\xi+\Delta\xi} - Q_\xi}{\Delta\xi} = 0\,, \end{aligned} \tag{A 7}$$

$$\frac{\Lambda_{\xi+\Delta\xi} - \Lambda_\xi}{\Delta\xi} + \frac{\eta M}{L'}\,(\varepsilon_N - \varepsilon_M)\exp(\xi - \Lambda) = 0\,, \tag{A 8}$$

$$\frac{\Xi_{\xi+\Delta\xi} - \Xi_\xi}{\Delta\xi} + \frac{\eta M}{4\pi\varrho}\exp(\xi - 3\,\Xi) = 0\,, \tag{A 9}$$

$$\begin{aligned} \frac{\Theta_{\xi+\Delta\xi} - \Theta_\xi}{\Delta\xi} &- \frac{3\,\varkappa\,\eta M}{64\pi^2 ac}\big(L'(\exp(\Lambda) - 1) - L_{rc}\big) \\ &\times \exp(\xi - 4\,\Xi - 4\,\Theta) = 0\,, \end{aligned} \tag{A 10}$$

$$\frac{\Xi_{\xi,t} - \Xi_{\xi,t-\Delta t}}{\Delta t} - \varphi^{-1}\,\Phi_{\xi,t} + (1 - \varphi^{-1})\,\Phi_{\xi,t-\Delta t}\,. \tag{A 11}$$

Before Eq. (A 8) was formulated, the time derivatives of the functions U and V in Eq. (2) were expressed by time derivatives of the dependent variables P and T, using the definitions of U and V as given by Eqs. (5) and (6). These time derivatives were then joined to form a single term ε_M, the mechanical work that is generated per gram and per second. In difference form ε_M in Eq. (A 8) thus becomes:

$$\varepsilon_M = -(4\,\beta^{-1} - 3)\,V P\,(D_{\Psi,t} - \nabla_{\rm ad}^{-1}\,D_{\Theta,t}) \tag{A 12}$$

where

$$D_{\Psi,t} = \frac{\varphi}{\Delta t}(\Psi_t - \Psi_{t-\Delta t}) - (\varphi - 1)\,D_{\Psi,t-\Delta t} \tag{A 13}$$

and

$$D_{\Theta,t} = \frac{\varphi}{\Delta t}(\theta_t - \theta_{t-\Delta t}) - (\varphi - 1)\, D_{\Theta, t-\Delta t}\,. \qquad \text{(A 14)}$$

Analogous $D_{\Phi,t}$ in Eq. (A 7) is defined by

$$D_{\Phi,t} = \frac{\varphi}{\Delta t}(\Phi_t - \Phi_{t-\Delta t}) - (\varphi - 1)\, D_{\Phi, t-\Delta t}\,. \qquad \text{(A 15)}$$

The constant φ in Eqs. (A 11), (A 13), (A 14) and (A 15) determines the phase shift between the time differences and the dependent variables. Either the value $\varphi = 1$ (meaning backward time differences) or the value $\varphi = 2$ (centered time differences) was used.

In Eqs. (A 7) through (A 10) all dependent variables and functions where the mass argument ξ is not indicated explicitly by a subscript, are mean values of the corresponding two values at ξ and at $\xi + \Delta\xi$. The time argument in these four equations is always t.

A disadvantage of the difference scheme described above is that numerical difficulties may be encountered when the energy dissipation by the artificial viscosity is included in Eq. (A 8) by adding an additional term ε_Q. This happens because at a given time t the artificial viscosity characteristically adds heat to only about 2 to 4 mass shells (over which the shock front is smoothed out). In these shells the internal energy and thus the temperature is increasing with time. But since in the difference scheme the dependent variables are not defined for the mass shell itself but for the boundaries of the shell only, an increase of T in the shell means that the mean of the two temperature values at the two boundaries of the mass shell is increased. The difficulty now is that the boundaries of each mass shell are also boundaries of the two neighboring mass shells. Let us assume e.g. that because of $\varepsilon_Q \neq 0$ in the n^{th} mass shell the temperature at the boundary between the n^{th} and the $(n+1)^{\text{st}}$ mass shell is increased. Let us further assume that in the $(n+1)^{\text{st}}$ mass shell we have $\varepsilon_Q = 0$ and that therefore in this shell in order to satisfy the energy law the mean of the temperature values at the two boundaries must stay constant. Then, since T at the boundary between the n^{th} and the $(n+1)^{\text{st}}$ shell is increased, the temperature at the boundary between the $(n+1)^{\text{st}}$ and the $(n+2)^{\text{nd}}$ shell has to decrease. Because of the same reasons (and assuming that $\varepsilon_Q = 0$ for all following mass shells) T at the boundary between the $(n+2)^{\text{nd}}$ and the $(n+3)^{\text{rd}}$ shell must increase again correspondingly. And so on. Thus, including an ε_Q in Eq. (A 8) would result in sawtooth like solutions for the functions $T(M_r)$ [and $L_r(M_r)$]. Test calculations showed that in the presence of strong shock waves this effect may lead to erroneous solutions and to slow convergence or even divergence of the Henyey method. Therefore, for the present problem the energy dissipation by the artificial viscosity was treated in a different but energetically equivalent way, as described in the main text.

References

Beals, C.S. 1951, *Publ. Dom. Astroph. Obs. Victoria* **9**, 1.
Bodenheimer, P. 1968, *Ap. J.* **153**, 483.
Christy, R.F. 1964, *Rev. Mod. Phys.* **36**, 555.
Cox, A.N., Brownlee, R.R., Eilers, D.D. 1966, *Ap. J.* **144**, 1024.
De Groot, M. 1969, *Bull. Astr. Inst. Netherlands* **20**, 225.
Fernie, J.D. 1968, *Observatory* 88, 167.
Hazlehurst, J. 1962, The Shock-Wave Theory of Novae, in *Advances in Astronomy and Astrophysics*, Ed. Zdeněk Kopal, Academic Press, New York.
Henyey, L.G., Wilets, L., Böhm, K.H., LeLevier, R., Levee, R.D. 1959, *Ap. J.* **129**, 628.
Hofmeister, E., Kippenhahn, R., Weigert, A. 1964, *Z. Astrophys.* **59**, 215.
Hutchings, J.B. 1969, *Mon. Not. Roy. Astr. Soc.* **144**, 143.
Kippenhahn, R., Weigert, A., Hofmeister, E. 1967, Methods for Calculating Stellar Evolution, in *Methods in Computational Physics*, Vol. 7, Academic Press, New York, p. 129.
Kopylow, I.M. 1958, *Crim. Astrophys. Obs.* **20**, 156.
Kushwaha, R.S., Odgers, G.J. 1960, *Publ. Dom. Astroph. Obs. Victoria* **11**, No. 6, 185.
Ledoux, P. 1941, *Ap. J.* **94**, 537.
Luud, L.S. 1967, *Soviet Astr.* **11**, 211.
Magalashvili, N.L., Kharadse, E.K. 1967a Comm. 27 I.A.U. Inf. Bull. Var. Stars No. 210.
Magalashvili, N.L., Kharadse, E.K. 1967b, *Observatory* 87, 295.
Müller, G., Hartwig, E. 1920, Geschichte und Literatur des Lichtwechsels veränderlicher Sterne, Vol. II, Poeschel & Trepte, Leipzig, p. 444.
Myschkis, A.D. 1955, Lineare Differentialgleichungen mit nacheilendem Argument, VEB Deutscher Verlag der Wissenschaften, Berlin.
Richtmyer, R.D. 1957, Difference Methods for Initial Value Problems, Interscience Publishers, New York.
Sahade, J. ed. 1962, Symposium on Stellar Evolution, National University of La Plata, La Plata, p. 185.
Schwarzschild, M., Härm, R. 1959, *Ap. J.* **129**, 637.
Sparks, W.M. 1969, *Ap. J.* **156**, 569.
Stothers, R. 1966, *Ap. J.* **144**, 959.

I. Appenzeller
Universitäts-Sternwarte
BRD 3400 Göttingen, Geismarlandstr. 11,
Germany